

2-5-2019

Pentablock copolymer micelle nanoadjuvants enhance cytosolic delivery of antigen and improve vaccine efficacy while inducing low inflammation

Sujata Senapati

Iowa State University, sujata@iastate.edu

Ross J. Darling

Iowa State University, rdarling@iastate.edu

Darren Loh

Johns Hopkins University

Ian C. Schneider

Iowa State University, ians@iastate.edu

Michael J. Wannemeuhler

Follow this and additional works at: https://lib.dr.iastate.edu/chem_pubs

Iowa State University, mjwannem@iastate.edu

 Part of the [Biomaterials Commons](#), [Medical Pharmacology Commons](#), [Nanomedicine Commons](#), and the [Veterinary Toxicology and Pharmacology Commons](#)

See next page for additional authors

The complete bibliographic information for this item can be found at https://lib.dr.iastate.edu/chem_pubs/1105. For information on how to cite this item, please visit <http://lib.dr.iastate.edu/howtocite.html>.

This Article is brought to you for free and open access by the Chemistry at Iowa State University Digital Repository. It has been accepted for inclusion in Chemistry Publications by an authorized administrator of Iowa State University Digital Repository. For more information, please contact digirep@iastate.edu.

Pentablock copolymer micelle nanoadjuvants enhance cytosolic delivery of antigen and improve vaccine efficacy while inducing low inflammation

Abstract

As the focus has shifted from traditional killed or live, attenuated vaccines towards subunit vaccines, improvements in vaccine safety have been confronted with low immunogenicity of protein antigens. This issue has been addressed by synthesizing and designing a wide variety of antigen carriers and adjuvants, such as Toll-like receptor agonists (e.g., MPLA, CpG). Studies have focused on optimizing adjuvants for improved cellular trafficking, cytosolic availability, and improved antigen presentation. In this work, we describe the design of novel amphiphilic pentablock copolymer (PBC) adjuvants that exhibit high biocompatibility and reversible pH- and temperature-sensitive micelle formation. We demonstrate improved humoral immunity in mice in response to single dose immunization with PBC micelle adjuvants compared to soluble antigen alone. With the motive of exploring the mechanism of action of these PBC micelles, we studied intracellular trafficking of these PBC micelles with a model antigen and demonstrated that the PBC micelles associate with the antigen and enhance its cytosolic delivery to antigen presenting cells. We posit that these PBC micelles operate via immune-enhancing mechanisms that are different from that of traditional Toll-like receptor activating adjuvants. The metabolic profile of antigen presenting cells stimulated with traditional adjuvants and the PBC micelles also suggests distinct mechanisms of action. A key finding from this study is the low production of nitric oxide and reactive oxygen species by antigen presenting cells when stimulated by PBC micelle adjuvants in sharp contrast to TLR adjuvants. Together, these studies provide a basis for rationally developing novel vaccine adjuvants that are safe, that induce low inflammation, and that can efficiently deliver antigen to the cytosol.

Keywords

Adjuvant, Micelles, Block Copolymers, Antigen delivery, Antibody-mediated immunity, Immunometabolism

Disciplines

Biomaterials | Medical Pharmacology | Nanomedicine | Veterinary Toxicology and Pharmacology

Comments

This document is the unedited Author's version of a Submitted Work that was subsequently accepted for publication in *ACS Biomaterials Science and Engineering*, copyright © American Chemical Society after peer review. To access the final edited and published work see DOI: [10.1021/acsbiomaterials.8b01591](https://doi.org/10.1021/acsbiomaterials.8b01591).

Authors

Sujata Senapati, Ross J. Darling, Darren Loh, Ian C. Schneider, Michael J. Wannemeuhler, Balaji Narasimhan, and Surya K. Mallapragada

1
2
3
4 Pentablock copolymer micelle nanoadjuvants
5
6
7
8 enhance cytosolic delivery of antigen and improve
9
10
11
12 vaccine efficacy while inducing low inflammation
13
14
15
16
17

18 *Sujata Senapati^{1,4}, Ross J. Darling^{2,4}, Darren Loh³, Ian C.*
19
20 *Schneider^{1,4}, Michael J. Wannemuehler^{2,4}, Balaji Narasimhan^{1,4*}, and*
21
22 *Surya K. Mallapragada^{1,4,*}*
23
24
25
26
27
28

29 ¹Department of Chemical and Biological Engineering, Iowa State
30
31 University, Ames, IA, 50011, USA
32
33

34 ²Department of Veterinary Microbiology and Preventive Medicine,
35
36 Iowa State University, Ames, IA, 50011, USA
37
38
39

40 ³Department of Chemical and Biological Engineering, Johns Hopkins
41
42 University, Baltimore, MD, 21218, USA
43
44

45 ⁴Nanovaccine Institute, Iowa State University, Ames, IA, 50011,
46
47 USA
48
49

50
51 *Correspondence:
52

53
54 Surya Mallapragada (suryakm@iastate.edu) and Balaji Narasimhan (nbalaji@iastate.edu)
55
56

1
2
3
4
5
6
7
8
9
10
11
12
13
14
15
16
17
18
19
20
21
22
23
24
25
26
27
28
29
30
31
32
33
34
35
36
37
38
39
40
41
42
43
44
45
46
47
48
49
50
51
52
53
54
55
56
57
58
59
60

1
2
3 ABSTRACT
4
5
6

7 As the focus has shifted from traditional killed or live,
8 attenuated vaccines towards subunit vaccines, improvements in
9 vaccine safety have been confronted with low immunogenicity of
10 protein antigens. This issue has been addressed by synthesizing
11 and designing a wide variety of antigen carriers and adjuvants,
12 such as Toll-like receptor agonists (e.g., MPLA, CpG). Studies
13 have focused on optimizing adjuvants for improved cellular
14 trafficking, cytosolic availability, and improved antigen
15 presentation. In this work, we describe the design of novel
16 amphiphilic pentablock copolymer (PBC) adjuvants that exhibit high
17 biocompatibility and reversible pH- and temperature-sensitive
18 micelle formation. We demonstrate improved humoral immunity in
19 mice in response to single dose immunization with PBC micelle
20 adjuvants compared to soluble antigen alone. With the motive of
21 exploring the mechanism of action of these PBC micelles, we studied
22 intracellular trafficking of these PBC micelles with a model
23 antigen and demonstrated that the PBC micelles associate with the
24 antigen and enhance its cytosolic delivery to antigen presenting
25 cells. We posit that these PBC micelles operate via immune-
26 enhancing mechanisms that are different from that of traditional
27 Toll-like receptor activating adjuvants. The metabolic profile of
28 antigen presenting cells stimulated with traditional adjuvants and

1
2
3 the PBC micelles also suggests distinct mechanisms of action. A
4
5 key finding from this study is the low production of nitric oxide
6
7 and reactive oxygen species by antigen presenting cells when
8
9 stimulated by PBC micelle adjuvants in sharp contrast to TLR
10
11 adjuvants. Together, these studies provide a basis for rationally
12
13 developing novel vaccine adjuvants that are safe, that induce low
14
15 inflammation, and that can efficiently deliver antigen to the
16
17 cytosol.
18
19
20
21
22
23
24

25 KEYWORDS

26
27
28 Adjuvant, Micelles, Block Copolymers, Antigen delivery, Antibody-
29
30 mediated immunity, Immunometabolism
31
32
33
34
35
36
37
38
39
40
41
42
43
44
45
46
47
48
49
50
51
52
53
54
55
56
57
58
59
60

1
2
3 INTRODUCTION
4

5 Adjuvants have been used for almost seven decades to augment
6 immune responses to antigens in subunit vaccines¹⁻⁴. However, only
7 a few, such as alum and monophosphoryl lipid A (MPLA), are
8 currently approved by the United States Food and Drug
9 Administration for use in human vaccines⁵. These adjuvants suffer
10 from several limitations, including high reactogenicity, failure
11 to provide cell-mediated immunity, and variability in the
12 induction of immune responses in older adults⁶⁻⁸. Most vaccines or
13 adjuvants that are currently approved or in pre-clinical trials
14 work by the stimulation of pathogen recognition receptors (PRRs)
15 on antigen presenting cells (APCs). This leads to the induction of
16 inflammatory signals, such as cytokines, superoxides, and nitric
17 oxide (NO)⁵. However, due to immunosenescence in older adults, this
18 cytokine milieu is highly imbalanced leading to a state of
19 "inflamm-aging" and an overproduction of harmful oxide analytes^{9,10}.
20 While the traditional approach for vaccine design works in most
21 cases, the presence of inflammaging in older adults necessitates
22 the development (and exploration of mechanism of action) of novel
23 vaccine adjuvants that do not induce the production of harmful
24 analytes while stimulating the immune system.
25
26
27
28
29
30
31
32
33
34
35
36
37
38
39
40
41
42
43
44
45
46
47
48
49

50 A significant amount of research has been focused on improving
51 transport and delivery of antigens and adjuvants to APCs^{11,12}. These
52 antigens can be processed by APCs and presented via MHC I or MHC
53
54
55
56
57
58
59
60

1
2
3 II pathway for the induction of effective T and B cell responses¹².
4
5 Studies have focused on pH-sensitive amphiphilic polymer-based
6
7 vaccine delivery vehicles to enhance antigen presentation to the
8
9 MHC I pathway and to induce CD8⁺ T cell responses that can be
10
11 beneficial for enhancing the breadth of protection against
12
13 intracellular pathogens¹³⁻¹⁵. In particular, cationic polymeric
14
15 systems have been shown to enhance endosomal escape of the antigen
16
17 due to the proton sponge effect and enhance cytosolic uptake of
18
19 the antigen¹⁶⁻¹⁸.
20
21
22

23 Amphiphilic pentablock copolymers based on Pluronic F127®,
24
25 poly(ethylene oxide) (PEO) and poly(propylene oxide) (PPO), and
26
27 cationic blocks such as poly(diethylaminoethylmethacrylate)
28
29 (PDEAEM) have been previously studied for drug delivery and gene
30
31 delivery¹⁹⁻²¹. Aqueous solutions of these polymers can form
32
33 spherical micelles (about 30 nm in diameter) and at higher
34
35 concentrations (>20 wt.% polymer) form physical hydrogels in
36
37 response to both temperature and pH^{22,23}. The observation that small
38
39 particle sizes of antigen delivery systems can enhance
40
41 internalization by APCs has been widely exploited by different
42
43 nanoparticle systems²⁴⁻²⁷. Therefore, a polymer system having both
44
45 sub-100 nm size and stimuli responsiveness can be extremely
46
47 beneficial. Hydrogels based on these pentablock copolymers (PBC)
48
49 have been shown to provide sustained release of structurally stable
50
51
52
53
54
55
56
57
58
59
60

1
2
3 antigen *in vivo* and enhance anti-ovalbumin (Ova) antibody
4 responses^{28,29}. We have also demonstrated in previous influenza
5 virus challenge experiments that these PBC formulations can
6 enhance neutralizing antibody titers that effected a reduction in
7 viral load in lungs and exhibit improved vaccine efficacy in mice³⁰.
8
9 In this study, we prepared low concentration PBCs in aqueous
10 solutions to form micelles without gelation that still enhanced
11 antibody responses. This also eliminates any potential
12 inflammatory responses associated with the high polymer
13 concentrations needed to form gels³¹. However, little is known
14 about the mechanism of action of PBC micelle adjuvants; how they
15 interact with innate immune cells; and how these interactions lead
16 to the induction of effective adaptive immunity.
17
18
19
20
21
22
23
24
25
26
27
28
29
30
31

32 In this work, to explore the mechanism of action of these PBC
33 micelles, we characterized antigen-micelle complexes using Forster
34 Resonance Energy Transfer (FRET) spectroscopy and microscopy and
35 showed that Ova associated with the micelles in the solution phase
36 and that the PBC micelles enhanced Ova delivery to the cytosol *in*
37 *vitro* in APCs. We also studied the stimulation of APCs with
38 antigen-containing PBC micelles using three different approaches.
39 In the first phase, we analyzed the upregulation of co-stimulatory
40 molecules and cytokine secretion profile from APCs. Next, we
41 measured the oxygen consumption rate by the mitochondria of APCs
42
43
44
45
46
47
48
49
50
51
52
53
54
55
56
57
58
59
60

1
2
3 as a measure of stimulation. We analyzed the mitochondrial
4
5 respiration and metabolic profile in comparison to the TLR agonist
6
7 lipopolysaccharide (LPS). Finally, we studied the amount of innate
8
9 effector molecule (such as NO and reactive oxygen species (ROS))
10
11 secretion by APCs upon stimulation with PBC micelles.
12
13 Collectively, the studies presented here focus on the analysis of
14
15 the responses of innate immune cells stimulated by novel PBC
16
17 micelle adjuvants in order to understand their mechanism of action
18
19 so as to develop safe and effective adjuvants with low inflammatory
20
21 potential.
22
23
24
25
26
27
28
29
30
31
32
33
34
35
36
37
38
39
40
41
42
43
44
45
46
47
48
49
50
51
52
53
54
55
56
57
58
59
60

EXPERIMENTAL SECTION

Materials

N,N-(diethylamino)ethyl methacrylate (DEAEM), Pluronic F127, Poly(vinyl alcohol) (PVA, MW=9,000-10,000 g/mol), and ovalbumin (Ova, 44 kDa) were purchased from Sigma-Aldrich (St. Louis, MO). Alum (Alhydrogel[®]) and dyes for imaging and labeling were purchased from InVivogen (San Diego, CA). All other materials were purchased from Fisher Scientific (Pittsburgh, PA).

Methods

Pentablock copolymer synthesis and characterization

Pentablock copolymer (PDEAEM-PEO-PPO-PEO-PDEAEM) was synthesized by atom transfer radical polymerization (ATRP) as reported previously²². This method utilizes a difunctional macroinitiator prepared from commercially available Pluronic[®] F127. This was dissolved in tetrahydrofuran and reacted overnight with triethylamine and 2-bromoisobutyryl. The product was precipitated in n-hexane. The 2-bromo propionate Pluronic F127 was analyzed using ¹H NMR to confirm the end group functionalization. Next, the macroinitiator and the monomer DEAEM were used to synthesize the pentablock copolymer by ATRP utilizing copper (I) oxide nanoparticles as the catalyst and N-propylpyrrolidinemethanamine (NPPM) as the complexing ligand. Cuprous oxide nanoparticles used

1
2
3 as catalyst were synthesized as previously described³². ¹H NMR
4
5 spectra of the resulting polymer were used to determine molecular
6
7 weight.
8
9

10 11 12 Labeling of PBC and antigen with fluorescent dyes 13

14 The PBC and Ova were labeled with dyes to detect them
15
16 fluorescently. We utilized an Alexa Fluor 594 protein labeling kit
17
18 that utilizes a succinimidyl ester moiety to react with the primary
19
20 amines of the proteins (Molecular Probes, Eugene, OR) for labeling
21
22 ovalbumin according to the manufacturer's protocol. For labeling
23
24 the PBC we functionalized the end groups with azide following
25
26 previously described²⁸. We then utilized azide-alkyne click
27
28 chemistry to attach alkyne functionalized Alexa Fluor 647 (Thermo
29
30 Fisher Scientific, Waltham, MA) according to the manufacturer's
31
32 protocol.
33
34
35
36
37
38

39 40 PBC hydrogel and micelle formulations

41 A stock solution of 30% PVA was prepared in phosphate-buffered
42
43 saline (PBS). For the hydrogel formulation, this stock solution
44
45 was added to obtain a final concentration of 15 wt.% PVA, 5.9 wt.%
46
47 Pluronic® F127 and 4.1 wt.% PBC in PBS. For the micelle formulation,
48
49 a similar procedure was followed to obtain a final concentration
50
51 of 7.5 wt.% PVA, 2.95 wt.% Pluronic F127 and 2.05 wt.% PBC in PBS.
52
53
54
55

1
2
3 A micelle formulation with the fluorescently labelled PBC was also
4 prepared and used in experiments as required.
5
6
7
8
9

10 Animals

11 Female C57BL/6 or BALB/c mice (6-7-week-old) were purchased from
12 Charles River Laboratories (Wilmington, MA). The Institutional
13 Animal Care and Use Committee (IACUC) at Iowa State University
14 approved all protocols involving animals.
15
16
17
18
19
20
21
22

23 Immunizations and evaluation of antibody titers

24 To evaluate antibody responses, C57BL/6 or BALB/c mice were
25 subcutaneously immunized with 100 μ L of the micelle formulation,
26 100 μ L of hydrogel formulation, or alum in a 1:1 ratio with Ova,
27 all containing 50 μ g of Ova. Control animals were immunized with
28 soluble Ova in PBS (50 μ g in 100 μ L) (i.e., no adjuvant). Serum
29 samples were collected via the saphenous vein at 21 days and 35
30 days post-immunization. Enzyme-linked immunosorbent assay (ELISA)
31 was performed to measure the total anti-Ova total IgG titers.
32 Briefly, high binding 96-well ELISA plates were coated with Ova
33 overnight and blocked with 2% w/v gelatin (BD Difco™, Fisher
34 Scientific, Hampton, NH) in 0.05% Tween-PBS solution the following
35 day. Serum samples were added at a dilution of 1:200 and diluted
36 1:2 across the plate. After incubation and washing, alkaline-

1
2
3 phosphatase-conjugated anti-mouse IgG (H+L) (Jackson
4
5 ImmunoResearch, Westgrove, PA) was added and incubated for two
6
7 hours before adding substrate buffer and reading the plate at 405
8
9 nm. Titer was recorded as the last dilution that exhibited an
10
11 optical density greater than twice the background optical density.
12
13
14
15

16
17 Generation of bone marrow dendritic cells (BMDCs) and bone marrow
18
19 macrophages (BMMs)
20

21 Bone marrow was harvested from femurs and tibia of BALB/c mice
22
23 and differentiated to dendritic cells using a standard protocol³³.
24
25 Briefly, the bone marrow was flushed out of the bones using a
26
27 syringe with 5 mL of RPMI media containing 1% (1 g/100 mL)
28
29 pen/strep. Granulocyte macrophage colony stimulating factor (GM-
30
31 CSF) was added on the 1st day of culture at the concentration of
32
33 1ng/mL . GM-CSF and medium was refreshed on days 3, 6 and 8 of
34
35 culture by exchanging 10 mL of spent medium with fresh medium
36
37 containing GM-CSF. BMDCs were harvested on day 10 and used in
38
39 subsequent assays. The same protocol was followed for BMMs except
40
41 using DMEM medium and macrophage colony stimulating factor (M-CSF)
42
43 as the cytokine at a concentration of 1 ng/mL.
44
45
46
47
48
49
50

51 Confocal microscopy
52
53
54
55

1
2
3 J774 macrophage cell line and BALB/c-derived BMDCs were used to
4
5 analyze the cellular internalization of antigen-containing
6
7 micelles using confocal microscopy. Cells were cultured on and
8
9 allowed to adhere to round glass coverslips (VWR, Radnor, PA) in
10
11 24 well flat-bottom cell culture plates overnight. For J774s, since
12
13 they are adherent, no coating on the coverslips was used. However,
14
15 for the BMDCs we treated the coverslips with poly D-lysine for 12
16
17 hours before cell culture. The cells were incubated for 15 min, 30
18
19 min, 2 hours and 12 hours with the labeled Ova solution (20 µg/mL)
20
21 and the micelle formulation (12.5 µg/mL) consisting of labeled
22
23 PBC, together and separately as controls. For the groups treated
24
25 with micelle-Ova complex, the micelle and Ova solutions were co-
26
27 incubated for an hour before adding them to the cells. The cells
28
29 were then stained with Hoescht 33342 solution for nuclear staining
30
31 (ThermoFisher Scientific) as described in the commercial protocol.
32
33 Anti-mouse LAMP-1 (1D4B) (Developmental Studies Hybridoma Bank,
34
35 University of Iowa) was used to stain lysosomes in BMDCs. The cells
36
37 were then fixed and the cover slips were mounted on microscopic
38
39 slides (VWR, Radnor, PA). A Leica SB5 X MP confocal microscope was
40
41 used to image the cell samples and the images were analyzed using
42
43 LAS AF software (Leica Microsystems, Wetzlar, Germany).
44
45
46
47
48
49
50
51
52

53 FRET spectroscopy and microscopy
54
55
56
57
58
59
60

1
2
3 AF594 tagged to Ova and AF647 tagged to the PBC (Forster radius,
4 $R_0 = 8.5$ nm) acted as the donor and acceptor fluorophore,
5 respectively for FRET analysis. Solutions with 12.5 $\mu\text{g/mL}$ of PBC
6 micelle formulation and 20 $\mu\text{g/mL}$ of Ova were mixed together or
7 added separately to measure the fluorescence spectra using a dual
8 monochromator spectrofluorometer (Fluoromax-4, Horiba Jobin Yvon,
9 Kyoto, Japan) with slit width of 3 nm at the excitation of the
10 donor (590 nm) and emission wavelengths for the two fluorophores
11 (AF594 Em: 610 nm and AF647 Em: 660 nm).
12
13
14
15
16
17
18
19
20
21
22

23 For FRET microscopy, Leica SB5 X MP confocal microscope was used
24 for slides prepared in a similar manner as confocal microscopic
25 imaging using the same concentrations of the PBC micelle and Ova
26 solutions. However, the settings in the microscope were changed
27 according to the procedure used to measure sensitized emission for
28 FRET³⁴, which involves the measurement of acceptor emission change
29 with the addition of the donor. The different images taken in order
30 were: (a) FRET sample images in the FRET channel (donor excitation
31 and acceptor emission), donor channel (donor excitation and donor
32 emission), acceptor channel (acceptor excitation and acceptor
33 emission); (b) Acceptor only sample image in the acceptor channel;
34 and (c) Donor only sample image in the donor channel. The last two
35 images were taken to correct for the spectral bleed-throughs in
36 the channel to subtract the amount of radiation detected in the
37
38
39
40
41
42
43
44
45
46
47
48
49
50
51
52
53
54
55

1
2
3 FRET channel which is not due to the energy transfer. The
4
5 instrument settings were kept constant throughout the imaging. The
6
7 bleed-through was calculated using a linear regression obtained by
8
9 the FRET and colocalization analyzer plugin in ImageJ software
10
11 (NIH, Bethesda, MD). Final FRET index images, heat maps in the
12
13 "fire" Look-Up Table (LUT) and mean FRET indices were generated
14
15 by selecting regions of interest (ROIs) in the images where cells
16
17 were present.
18
19
20
21
22

23 *In vitro* APC stimulation

24
25 BALB/c-derived BMDCs, BMMs, and J774s were plated at 5×10^5
26
27 cells/well in a 96-well round bottom tissue culture plate in 200
28
29 μL of complete RPMI 1640 medium with 1% pen/strep (1 g/100 mL).
30
31 Stimulations were carried out overnight or for 48 hours using 12.5
32
33 $\mu\text{g/mL}$ of micelles, 1 $\mu\text{g/mL}$ of LPS, or untreated control wells.
34
35 Supernatants were collected for cytokine analysis and NO
36
37 quantification, and cells were harvested (using cell scrapers for
38
39 BMMs and J774s) for cell surface marker expression and mitochondrial
40
41 and cell superoxide production by flow cytometry.
42
43
44
45
46
47
48

49 Cytokine secretion assay

50
51 The cell-free supernatants collected after stimulating the
52
53 different cellular populations for 48 hours were used to evaluate
54
55

1
2
3 the levels of cytokine secretions. BioRad BioPlex 200 system
4
5 (Hercules, CA) was used to analyze IL-6, TNF- α , IL-1 β , IL-12 and
6
7 IFN γ secretions.
8
9

10 11 12 Flow cytometry

13
14 Costimulatory marker expression on APCs was evaluated using flow
15
16 cytometry. BMDCs at a concentration of 5×10^5 cells/200 μ L were
17
18 aspirated from a 96 well plate and transferred to polystyrene FACS
19
20 tubes. Prior to labeling with specific monoclonal antibodies, Fc
21
22 receptors on DCs were blocked to prevent non-specific antibody
23
24 binding by incubating the cells with 100 μ g/mL of rat IgG (Sigma
25
26 Aldrich, St. Louis, MO) and 10 μ g/mL of anti-CD16/32 (eBioscience).
27
28 Subsequently, APCs were stained with fluorescently conjugated
29
30 antibodies for CD80 (Biolegend, PerCP-Cy5.5, clone 16-10A1), CD86
31
32 (eBioscience, FITC, clone GL1), CD40 (eBioscience, APC, clone
33
34 1C10), CD11c (Biolegend, APC-Cy7, clone N418), MHCII (eBioscience,
35
36 AF700, clone M5/114.15.2) diluted at 1:50 v/v in FACS buffer .
37
38
39
40

41
42 Mitochondrial superoxide production was evaluated using live
43
44 cells stained with MitoSOX Red (ThermoFisher Scientific) according
45
46 to manufacturer's specifications. The amount of reactive oxygen
47
48 species (ROS) produced by the BMDCs was measured using CellROX
49
50 Green (ThermoFisher Scientific) according to the manufacturer's
51
52 protocol.
53
54
55

1
2
3 Fluorescent activated cell sorting (FACS) was used to quantify
4
5 the internalization of protein and micelles into BMDCs and a
6
7 macrophage cell line J774. The cells were treated with either the
8
9 labeled Ova (20 µg/mL) or the PBC micelles (12.5 µg/mL) , or the
10
11 micelle-Ova complex obtained after an hour of incubation of the
12
13 solutions, for multiple time intervals (15 min, 30 min, 2 hours
14
15 and 12 hours). After the incubation, the cells were transferred to
16
17 FACS tubes and suspended and washed in FACS buffer to remove the
18
19 excess dye not taken up by the cells. All the samples for flow
20
21 cytometry except the MitoSOX and CellROX samples were fixed using
22
23 BD stabilizing fixative (BD Bioscience, Franklin Lakes, NJ). Data
24
25 was collected on a FACSCanto II (BD Bioscience, Franklin Lakes,
26
27 NJ), and analyzed using FlowJo (Flowjo LLC, Ashland, OR).

32 33 34 35 Extracellular flux analysis

36
37 Metabolic effect of stimulation of BMDCs was measured using two
38
39 assays. For measurement of oxidative phosphorylation, the oxygen
40
41 consumption rate (OCR) was analyzed by performing an overnight
42
43 stimulation of BMDCs with either 12.5 µg/mL of PBC micelles, 1
44
45 µg/mL of LPS, or untreated control, was carried out in 5 mL
46
47 polypropylene tubes. 2.5×10^5 stimulated BMDCs were seeded into
48
49 Cell-Tak (Corning, Corning NY) coated Seahorse plates and a
50
51 mitochondrial stress test (MST) was conducted according to
52
53
54
55

1
2
3 manufacturer's specifications using kit concentrations of 1 μM
4 oligomycin, 2 μM FCCP, and 0.5 μM rotenone and antimycin (Agilent,
5 Santa Clara, CA).
6
7

8
9
10 For measurement of acute metabolic responses and glycolysis
11 (demonstrated by extracellular acidification rate, ECAR) upon
12 stimulation, untreated BMDCs were seeded into Cell-Tak (Corning,
13 Corning NY) coated seahorse plates at a density of 2.5×10^5
14 untreated BMDCs per well. Baseline metabolic activity readings
15 were measured, and wells were stimulated with 12.5 $\mu\text{g}/\text{mL}$ of
16 micelle, 1 $\mu\text{g}/\text{mL}$ of LPS, or medium control and metabolic
17 measurements are taken over the course of the assay. All metabolic
18 phenotyping was conducted on a Seahorse XFe24 (Agilent, Santa
19 Clara, CA).
20
21
22
23
24
25
26
27
28
29
30
31
32
33
34

35 Nitric oxide quantification

36
37 Nitric oxide (NO) in supernatants obtained from BMDCs, BMMs and
38 J774 cells stimulation for 48 hours was quantified using a Griess
39 assay. A sodium nitrite standard curve was created with
40 concentrations ranging from 100 μM to 0 μM . 100 μL of Griess
41 reagent (Cat. No. 03553, Sigma-Aldrich) was added to 100 μL of
42 standard or sample supernatant in a 96 well microtiter plate.
43
44 Samples were allowed to react for 15 minutes at room temperature
45 and read at 540 nm on a SpectraMAX 190 (Molecular Devices,
46
47
48
49
50
51
52
53
54
55

1
2
3 Sunnyvale, CA) plate reader. Experimental nitrite concentrations
4
5 were calculated using a linear regression method.
6
7
8
9

10 Statistics

11 For the antibody titer data, statistical significance was
12 determined using One-way ANOVA and Tukey-post *t* test on the log 2
13 transformed titers using GraphPad (Prism 7.0, GraphPad Software,
14 La Jolla, CA). For all other experiments, statistical significance
15 was determined using one-way ANOVA analysis of the respective
16 values using GraphPad and *p*-values ≤ 0.05 were considered
17 significant.
18
19
20
21
22
23
24
25
26
27
28
29

30 Results

31 PBC micelle nanoadjuvant enhances antibody-mediated immunity

32 The ATRP method yielded PBC with outer cationic PDEAEM blocks
33 having a molecular weight of 14,680 g/mol as determined by ¹H NMR.
34 The micelle formulation prepared from PBC was administered to mice
35 with Ova to evaluate the induction of humoral immune responses. In
36 addition, separate groups of mice were administered either soluble
37 ovalbumin (sOVA), alum+Ova or a hydrogel formulation (as used in
38 previous studies), all containing 50 μ g of Ova²⁹. We observed a
39 nine-fold increase in anti-Ova antibody titers in sera of mice
40
41
42
43
44
45
46
47
48
49
50
51
52
53
54
55
56
57
58
59
60

immunized with micelles when compared to sOVA at two weeks post-immunization (p.i.) (Figure 1).

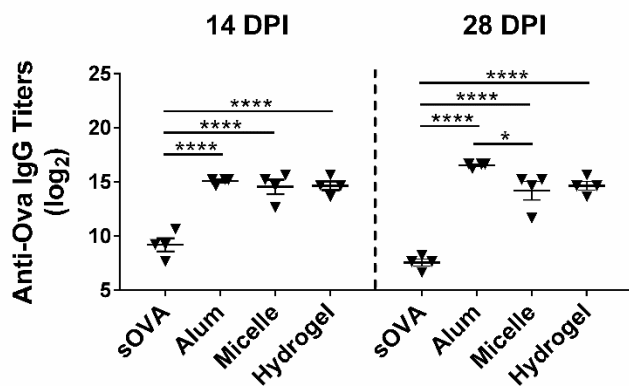


Figure 1. Pentablock copolymer (PBC) micelles enhanced antibody titers in C57BL/6 mice 2- and 4-weeks post-immunization. Serum collected at 14 and 28 dpi were used to evaluate anti-OVA total IgG titers using ELISA. Statistical differences between the treatment groups within each time-point were determined using one-way ANOVA and Tukey-post *t* test on the log 2 transforms of the titer dilution values. * indicates $p < 0.05$ and **** indicates $p < 0.0001$. Data are representative of two independent experiments with C57BL/6 mice and one independent experiment with BALB/c mice with 4-5 animals in each experiment per treatment group.

This fold-increase was sustained through four weeks p.i. In addition, we observed a significant increase in anti-OVA antibody titers in sera of animals immunized with the hydrogel formulation over the sOVA, consistent with our previous studies²⁹. However,

1
2
3 there were no significant differences observed between the micelle
4 and hydrogel formulations, indicating that the PBC micelle
5 enhanced humoral immunity even at much lower polymer concentration
6 (compared to the hydrogel formulation). This suggests that the
7 thermogelation or depot formation of the PBC hydrogel at the site
8 of injection is not the only mechanism of action of this adjuvant.
9
10 We also observed that the antibody titers in the animals immunized
11 with alum+Ova, which were not significantly different from the
12 titers induced in the animals immunized with PBC micelles at two
13 weeks p.i, became significantly different (about four-fold higher)
14 at four weeks p.i. We also performed anti-Ova IgM titers (data not
15 shown) that showed similar trends as IgG.
16
17
18
19
20
21
22
23
24
25
26
27
28
29
30
31

32 PBC micelle nanoadjuvants exhibit cytosolic uptake of antigen by
33 BMDCs and J774 cells
34

35
36
37 To understand the mechanism of the action of these PBC micelles
38 and identify factors that may contribute to the enhancement in
39 humoral immunity when immunized with micelles, we decided to first
40 probe their interaction with the APCs. Internalization of proteins
41 or peptides by the APCs is the first step in the triggering of
42 immune signaling to generate an immune response^{35,36}. We studied the
43 internalization of OVA-containing micelles by BMDCs and J774 cells
44 using confocal microscopy. We observed that the micelles (cyan)
45
46
47
48
49
50
51
52
53
54
55
56
57
58
59
60

1
2
3 and ovalbumin (red) were internalized efficiently by both the cell
4 types into the cytosol after a 30 min incubation time and stayed
5 the same until the 12-hour incubation time (Figure 2, SI Figure
6 2). However, we did not observe any internalization at the 15 min
7 time point (SI Figure 2). After 12 hours of incubation, we could
8 observe antigen in BMDCs co-localized with the lysosomes (showed
9 in green, Figure 2A). However, most of the antigen was distributed
10 across the cytosol indicating antigen release from the micelles.
11 In addition, due to their amphiphilic nature, we also observed a
12 large amount of micelles interacting with the cell membrane,
13 especially in the J774 cells starting at 15 min until after 12
14 hours of incubation. We also analyzed the cells that had
15 incorporated micelles using FACS. Almost 100% of the BMDCs and
16 J774 cells were positive for the micelles as soon as 15 min and
17 the labeling remained stable for at least 12-hours as indicated by
18 the clear shifts in the population in the flow cytometry plots (SI
19 Figure 1). The mean fluorescence intensity (MFI) of the micelle-
20 positive cell population however, increased from 15 min to 12 hours
21 for both BMDCs and J774 cells.
22
23
24
25
26
27
28
29
30
31
32
33
34
35
36
37
38
39
40
41
42
43
44
45
46
47
48
49
50
51
52
53
54
55
56
57
58
59
60

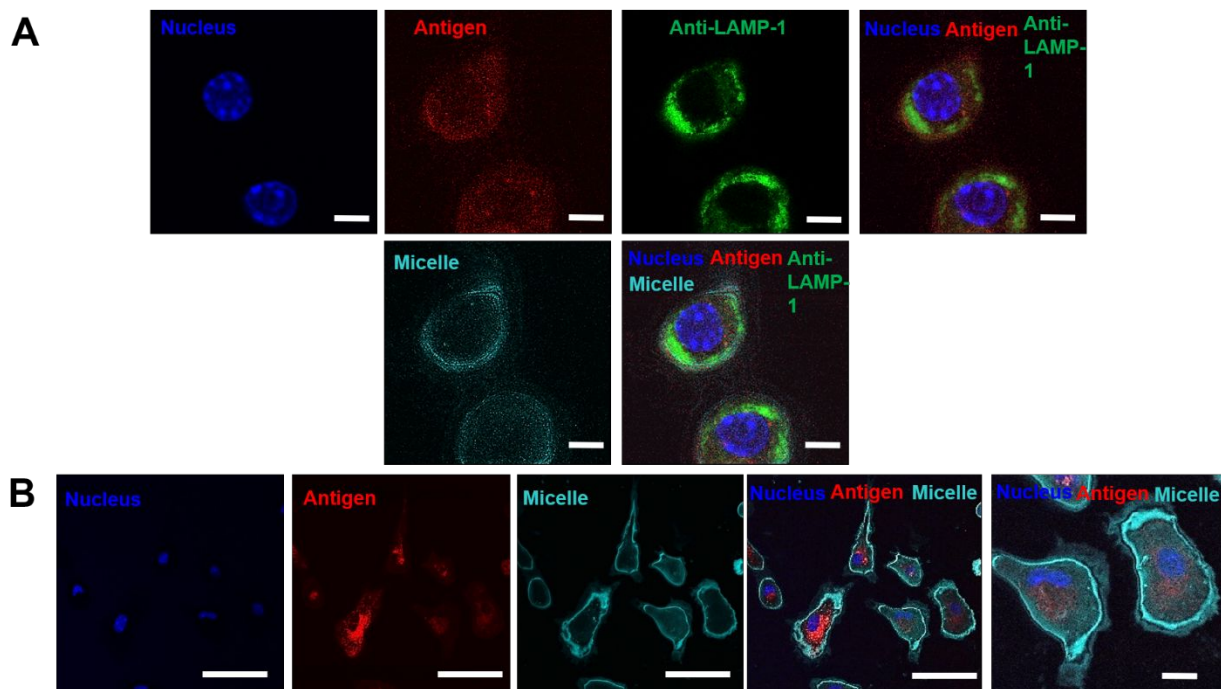
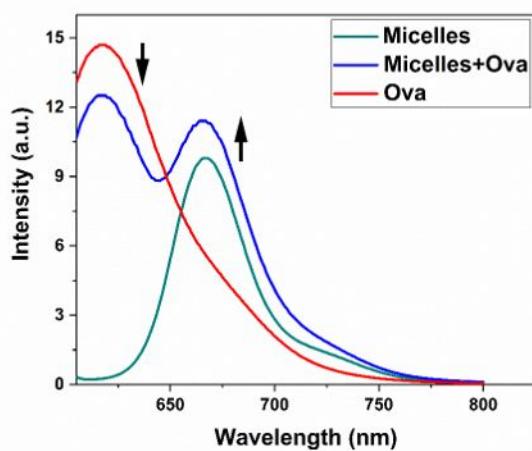


Figure 2. Pentablock copolymer (PBC) micelles efficiently traffic antigen to the cytosol. A) Bone marrow derived dendritic cells (BMDCs) and B) J774 cells were incubated with micelles and ovalbumin (i.e., antigen) for 12 hours over glass coverslips. Cell components were stained following the incubation and cells were fixed and transferred to glass slides for imaging. Scale bars indicate 5 μm in A and 50 μm and 5 μm in the first four and last columns of B, respectively. Nuclei were stained with Hoescht (blue), lysosomes were stained with anti-LAMP-1 (green). Ovalbumin antigen (AF594) and PBC micelles (AF647) are denoted by red and cyan, respectively. Data are representative of four independent experiments.

PBC micelle nanoadjuvants associate with antigen and enhance their uptake

Next, we assessed the nature of interaction of the PBC micelles with the antigen using FRET. We first incubated micelles with Ova labeled with dyes that exhibit FRET in solution phase for 15 minutes and studied the fluorescence spectrum of three solutions: (a) micelles only, (b) Ova only, and (c) micelles + Ova. FRET occurs if the donor and acceptor fluorophores are spatially proximal (less than 10 nm)³⁷. Upon occurrence of FRET, we observed a decrease in the intensity of donor fluorescence (at 610 nm for the dye tagged with ovalbumin) and an increase of almost the same magnitude in the acceptor intensity (at 660 nm the dye tagged with the micelles) when both were in solution together, compared to when they were in solution separately (Figure 3). These observations showed that the micelles associate with the antigen in solution phase.



1
2
3 **Figure 3. Pentablock copolymer (PBC) micelles associated with**
4 **ovalbumin in solution phase.** Micelles (12.5 mg/mL) and ovalbumin
5 (20 mg/mL) were labelled with AF647 and AF594, respectively. The
6 fluorescence spectra were measured for micelles only, ovalbumin
7 only, and micelles plus ovalbumin mixtures. Arrows indicate
8 decrease in AF594 (donor) fluorescence and increase in AF647
9 (acceptor) fluorescence.
10
11
12
13
14
15
16
17
18
19

20 We then evaluated whether the same phenomenon occurs in the
21 presence of immune cells. We incubated J774 cells and BMDCs with
22 micelles and Ova at different concentrations overnight and
23 included micelles-only and Ova-only controls. After removal of
24 spectral bleed-throughs and analysis of the images as described in
25 the Methods section, we obtained mean FRET indices. We observed
26 the highest FRET indices for a polymer concentration of 12.5 $\mu\text{g/mL}$
27 and protein concentration of 25 $\mu\text{g/mL}$ (mean FRET index = 16.8 for
28 BMDCs and = 9.6 for J774 cells, generated using the histograms) as
29 shown in Figures 4A and 4B. The images generated by the FRET
30 analyzer plug-in provided us with an estimate of the degree of
31 FRET occurring³⁴. We observed greater FRET (as indicated by the
32 color in the images and the heat map) in BMDCs than in J774 cells.
33 We also observed some areas of very high FRET in both cell types
34 (indicated by magenta color in the images).
35
36
37
38
39
40
41
42
43
44
45
46
47
48
49
50
51
52
53
54
55
56
57
58
59
60

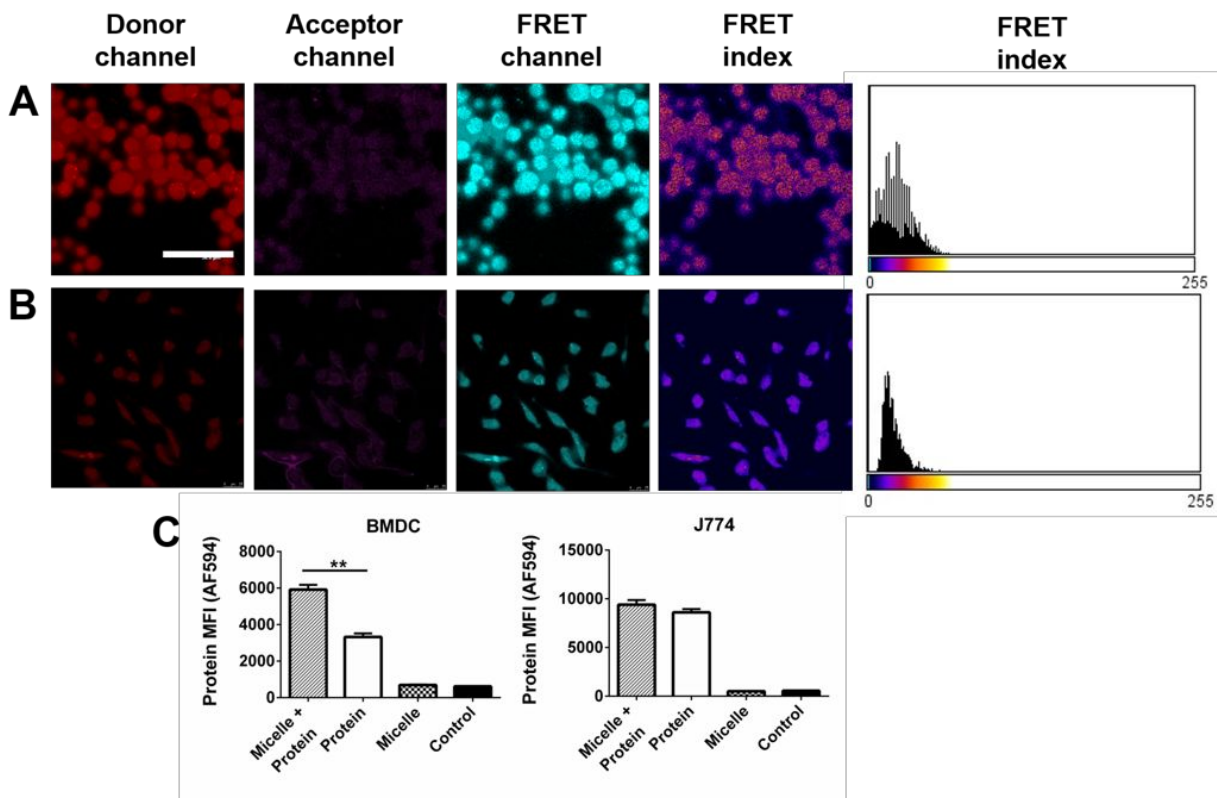


Figure 4. Pentablock copolymer (PBC) micelles associated with ovalbumin intracellularly and enhanced the uptake of ovalbumin in BMDCs. FRET microscopic analysis of A) BMDCs and B) J774 cells demonstrated strong association of micelles with protein with FRET indices of 16.8 and 9.6 respectively. Histograms in the far right represent the mean FRET indices with the heat map for the 'fire' Look-Up Table (LUT) used in the FRET index images. Excitation and emission wavelengths (Ex/Em) used to image are: Donor channel: 590 nm/620 nm, Acceptor channel: 650 nm/665 nm and FRET channel: 590 nm/665 nm. C) Ovalbumin uptake was increased two-fold when delivered with micelles in BMDCs. Statistical significance was determined using unpaired t test. ** indicates $p < 0.002$.

1
2
3 We hypothesized that the association of the micelles with antigen
4 may assist the antigen being carried into the cytosol. Therefore,
5 we performed FACS with J774 cells and BMDCs stimulated with
6 micelles and ovalbumin at the same concentration at which we
7 observed the highest FRET. We observed about a two-fold increase
8 in the antigen mean fluorescence intensity (MFI) when the BMDCs
9 were incubated with both the micelles and antigen than with the
10 antigen alone after 12-hours of incubation (Figure 4C). The amount
11 of antigen delivered to the cells also increased from 15 min to 12
12 hours of incubation and we observed significantly more antigen at
13 the 1-hour and 2-hours incubation periods for BMDCs than after 15
14 min or 30 min of incubation. (SI Figure 3). We observed a slight
15 (although not significant) increase in antigen MFI when J774 cells
16 were used.

37 APC stimulation by PBC micelle nanoadjuvants

39 While these previous experiments provided us valuable information
40 about micelle-antigen interactions, an understanding of how immune
41 cells perceive the antigen when it is adjuvanted with micelles is
42 necessary. The activation of APCs such as DCs is an important part
43 of the induction of innate and adaptive immune responses. DCs are
44 activated by recognition of damage associated molecular patterns
45 (DAMPs) or microbial associated molecular patterns (MAMPs), and

1
2
3 undergo maturation and upregulate different cell surface
4 markers^{38,39}. To characterize the same, we assessed the expression
5 of CD40, CD80, CD86 and MHCII in BMDCs and BMMs using flow
6 cytometry when stimulated with PBC micelles for 48 hours. Overall,
7 we observed little to no significant upregulation of these markers
8 in BMDCs (Figure 5) or BMMs (SI Figure 4) with PBC micelles,
9 compared to negative controls. The positive control, LPS however,
10 induced significantly higher levels of these surface markers,
11 consistent with the literature⁴⁰.
12
13
14
15
16
17
18
19
20
21
22
23
24
25
26
27
28
29
30
31
32
33
34
35
36
37
38
39
40
41
42
43
44
45
46
47
48
49
50
51
52
53
54
55
56
57
58
59
60

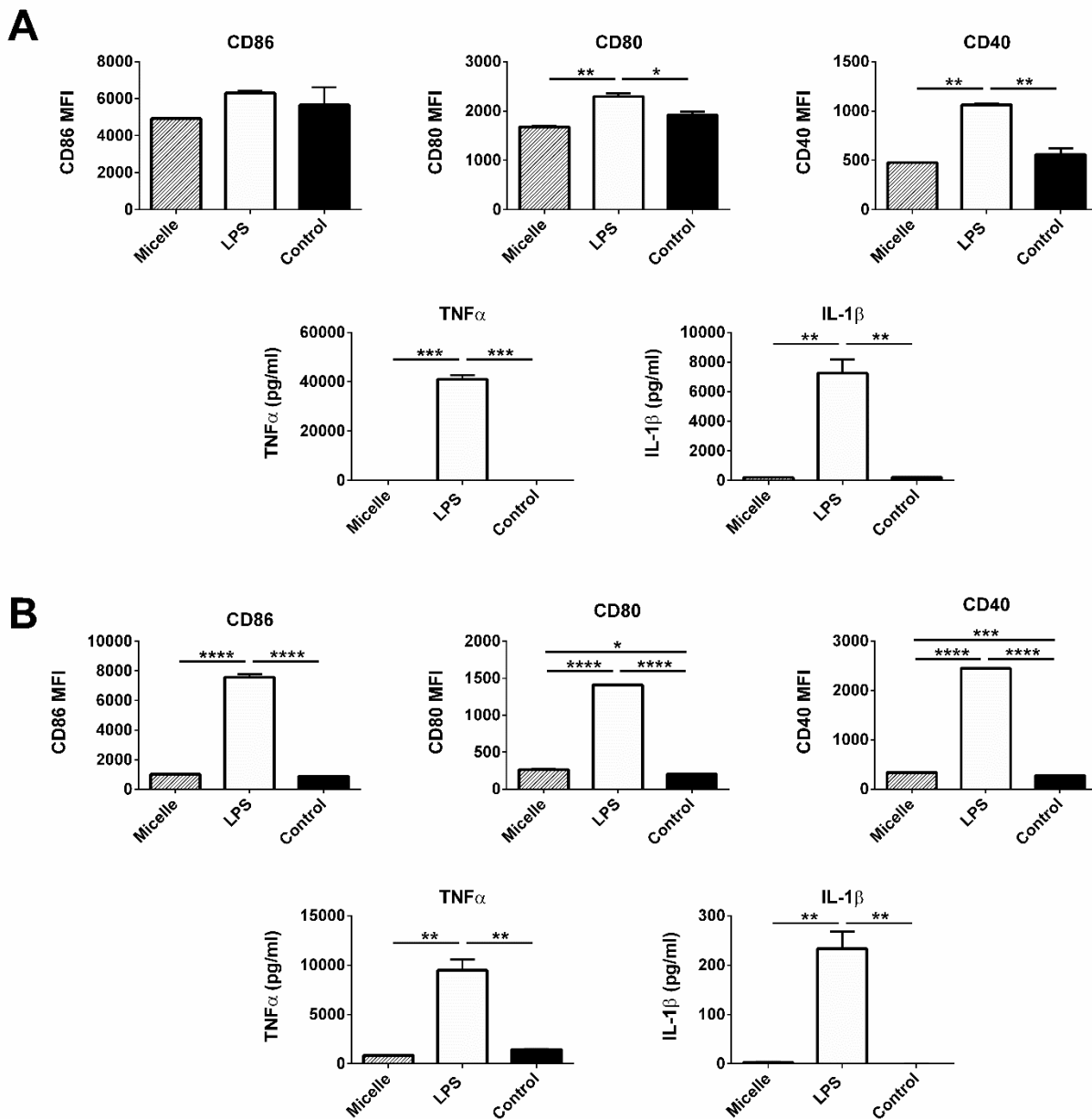


Figure 5. Pentablock copolymer (PBC) micelles did not activate innate immune cells as exhibited by cell surface markers expression and less inflammatory cytokines secretions. A) BALB/c-derived BMDCs and B) J774 cells at a concentration of 2.5×10^6 cells/mL were stimulated with different treatment groups (PBC micelles at the

1
2
3 concentration of 12.5 $\mu\text{g}/\text{mL}$ and LPS at 1 $\mu\text{g}/\text{mL}$) for 48 hours. Flow
4
5 cytometry was used to measure the cell surface marker upregulation.
6
7 Cytokine secretion was evaluated from the supernatants collected
8
9 after stimulation. Data is expressed as mean with standard error
10
11 of mean. Statistical differences were determined using one-way
12
13 ANOVA. *indicates $p < 0.05$, ** indicates $p < 0.005$ and *** indicates
14
15 $p < 0.0005$.
16
17
18
19

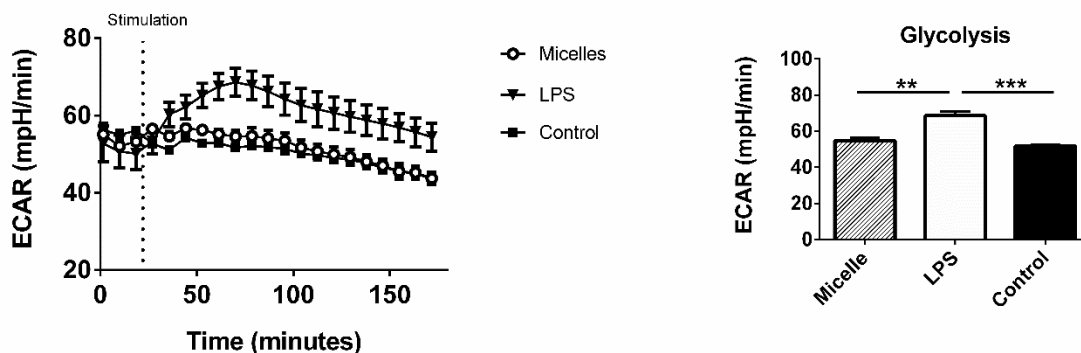
20 We also analyzed the levels of different cytokine secretions by
21
22 the APCs. The cytokine milieu often determines the fate of various
23
24 immune responses. We did not observe any secretion of the pro-
25
26 inflammatory cytokines, IL-6, TNF- α , IL-1 β , IL-12, IFN γ from BMDCs
27
28 and BMMs (Figure 5, SI Figure 4 and data not shown) in response to
29
30 the PBC micelle formulations. We observed very high levels of pro-
31
32 inflammatory cytokines secreted by APCs stimulated with LPS
33
34 (Figure 5 and SI Figure 2). Altogether, these data demonstrate the
35
36 low APC-stimulating characteristics of the PBC micelles unlike
37
38 traditional TLR-agonist adjuvants, such as LPS.
39
40
41
42
43
44

45 Immunometabolic profile of PBC micelle nanoadjuvants

46
47 Recent advances in the field of immunometabolism have described
48
49 the relationship between DC activation and the corresponding
50
51 metabolic changes⁴¹⁻⁴³. Several hours post-exposure to TLR ligands,
52
53 BMDCs exhibit a dramatic shift to a dependence on aerobic
54
55

1
2
3 glycolysis for survival and generation of ATP⁴⁴. This effect is
4
5 driven by the nitrosylation of electron transport chain (ETC)
6
7 molecules after production of large amounts of NO as a result of
8
9 encounter with TLR ligands⁴⁵. As a result, BMDCs exhibit a distinct
10
11 immediate glycolytic burst upon activation with TLR ligands. This
12
13 provides a rapid and sensitive method to detect whether BMDCs were
14
15 actively recognizing and responding to a particular adjuvant
16
17 formulation⁴⁶. Resting BMDCs were measured for baseline glycolytic
18
19 activity and then exposed to LPS, PBC micelle, or medium control.
20
21 Medium acidification rates were recorded as a measure of glycolytic
22
23 activity. Immediately upon exposure to LPS, BMDCs exhibited an
24
25 increase in glycolytic rate, while exposure to the micelle
26
27 formulation showed levels of glycolysis similar to the control
28
29 over the course of the assay (Figure 6A).
30
31
32
33
34
35
36
37
38
39
40
41
42
43
44
45
46
47
48
49
50
51
52
53
54
55
56
57
58
59
60

A



B

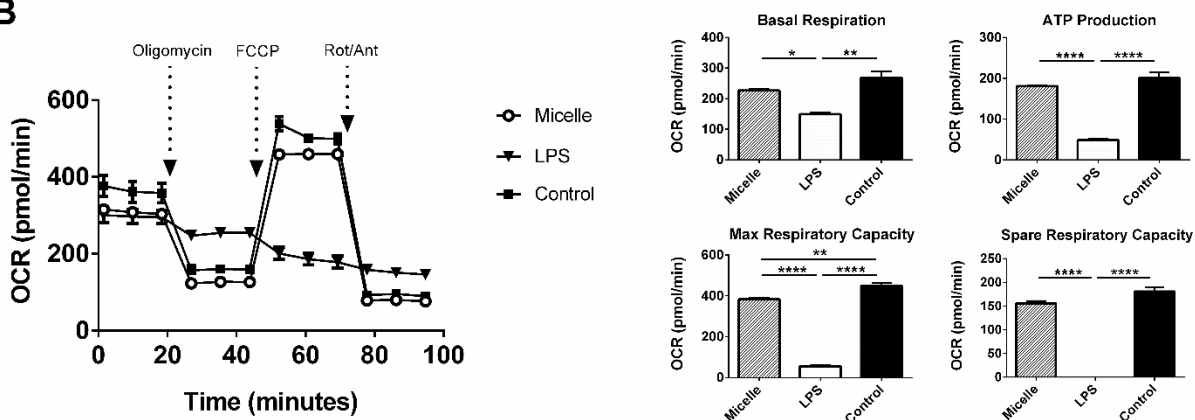


Figure 6. Treatment of BMDCs with pentablock copolymer (PBC) micelles did not induce a glycolytic shift in their metabolic profile. A) Kinetic stimulation test and B) Mitochondrial stress test for BMDCs stimulated with different treatment groups (PBC micelles at the concentration of 12.5 $\mu\text{g}/\text{mL}$ and LPS at 1 $\mu\text{g}/\text{mL}$) was performed overnight using extracellular flux analysis. Extracellular acidification rate (ECAR) and oxygen consumption rate (OCR) are represented by millipH/min and pmol/min. The figure on top right represents ECAR value at 61 minutes and figures in the bottom right represent different measures of the mitochondrial

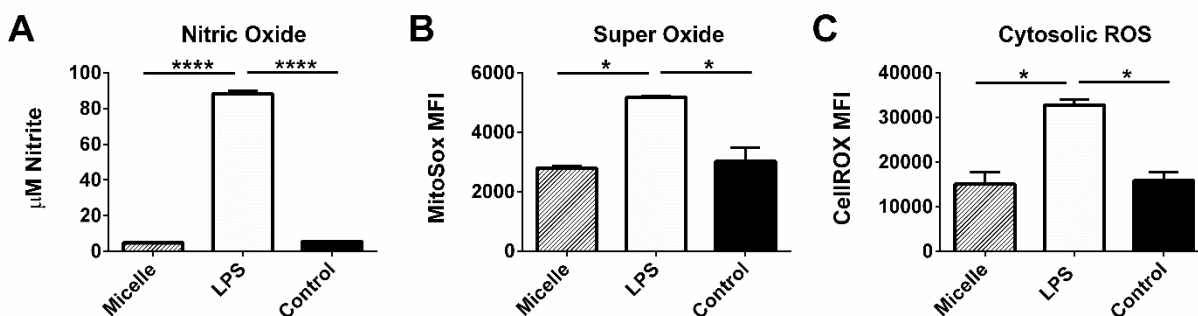
1
2
3 respiration derived from B as indicated in the text using standard
4
5 methods. * indicates $p < 0.02$, ** indicates $p < 0.002$ and *** indicates
6
7 $p < 0.0002$. $n = 2$.
8
9

10 To evaluate the metabolic consequences of exposure of BMDCs to
11
12 PBC micelles, we probed mitochondrial respiratory function with a
13
14 mitochondrial stress test (Figure 6B). Several parameters, such as
15
16 basal respiration, ATP production, maximum respiration and spare
17
18 capacity were measured using sequential injections of different
19
20 drugs⁴⁷. Addition of oligomycin, an inhibitor of ATP synthase,
21
22 complex V, provided the ATP production rate. The addition of FCCP,
23
24 which is a protonophore drives the ETC to function at its maximal
25
26 rate, provided the maximal and spare respiratory capacity of the
27
28 cells. Addition of rotenone, which shuts down the ETC provided the
29
30 rate of non-mitochondrial respiration to be subtracted. We found
31
32 that all these parameters for BMDCs stimulated with micelles were
33
34 not different from the control cells, while stimulation with LPS
35
36 led to decreased ATP turnover and decreased respiratory capacity
37
38 (Figure 6B).
39
40
41
42
43
44
45

46
47 PBC micelles do not induce detrimental ROS and NO production by
48
49 APCs
50

51 Upon encounter with a pathogen or MAMPs, cells of the innate
52
53 immune system induce the production of antimicrobial innate
54
55

1
2
3 effector molecules^{48,49}. These largely consist of various types of
4 reactive oxygen and reactive nitrogen species. Since little to no
5
6 reactive oxygen and reactive nitrogen species. Since little to no
7
8 upregulation of costimulatory molecules or increases in pro-
9
10 inflammatory cytokine secretion was exhibited in response to the
11
12 PBC micelles, we sought to determine if there was induction of ROS
13
14 and NO in APCs upon encounter with the micelles. NO production was
15
16 quantified from supernatants collected from BMDCs stimulated with
17
18 micelle, LPS, or unstimulated controls and quantified via Griess
19
20 assay. After 48 hours of stimulation, LPS stimulation resulted in
21
22 a marked accumulation of nitrite in the supernatants while PBC
23
24 micelle stimulation resulted in no accumulation of nitrite (Figure
25
26
27 7A). Similar results were observed in BMMs and J774 stimulations
28
29 (SI Figure 5). BMDCs were also analyzed for mitochondrial
30
31 superoxide and cytosolic ROS production. Similar patterns were
32
33 observed in that LPS induced the production of large amounts of
34
35 both superoxide and cytosolic ROS while stimulation with PBC
36
37 micelles resulted in no measurable increase in the production of
38
39 these molecules (Figures 7B and C).
40
41
42
43
44
45
46
47
48
49
50
51
52
53
54
55
56
57
58
59
60



1
2
3 **Figure 7. Pentablock copolymer (PBC) micelle adjuvants did not**
4 **induce the production of NO or ROS by APCs.** A) Nitric oxide
5
6 production by BMDCs, B) BMDC mitochondrial superoxide production,
7
8 and C) Reactive oxygen species production in the BMDC cytosol were
9
10 measured in the supernatants and cells stimulated with the
11
12 treatment groups (PBC micelles at the concentration of 12.5 µg/mL
13
14 and LPS at 1 µg/mL) for 48 hours using Griess assay and flow
15
16 cytometry. Data is expressed as mean with standard error of mean.
17
18 Statistical differences were determined using one-way ANOVA. *
19
20 indicates $p < 0.01$ and **** indicates $p < 0.0001$. n=3.
21
22
23
24
25
26
27
28

29 **Discussion**

30
31 Adjuvants have played a major role in enhancing vaccine
32
33 efficacy^{1,21,50}. The mechanisms of action of adjuvants range from
34
35 creating a depot, induction of inflammation, controlled release of
36
37 antigen, and acting as DAMPs. There has been a significant amount
38
39 of research on synthesizing new adjuvants, understanding their
40
41 mechanism(s) of action, and improving them for different
42
43 applications⁵¹. There are multiple viewpoints on the desirable
44
45 characteristics of next generation vaccine adjuvants⁵¹⁻⁵³. There is
46
47 a need to design new adjuvants and understand and exploit their
48
49 immunomodulatory properties to specifically suit certain types of
50
51
52
53
54
55
56
57
58
59
60

1
2
3 host immune systems, such as those of older adults and
4 immunocompromised patients.
5

6
7 In this work, we showed that amphiphilic PBC micelle-based
8 adjuvants can act as effective carriers for enhanced delivery of
9 antigens to APCs and induce robust adaptive immunity without the
10 production of NO and superoxides linked to the generation of an
11 overt inflammation. Hydrogels formed by PDEAEM and Pluronic F127®-
12 based PBCs have been previously demonstrated to induce robust
13 antibody responses as vaccine adjuvants and vaccines formulated
14 with these materials effectively protected animals against viral
15 challenge^{29,54}. In the present work, we demonstrated that immunizing
16 animals (C57BL/6 mice) with PBC micelles, at a significantly lower
17 polymer concentration than previously reported⁵⁵, enhanced anti-
18 Ova antibody titers in mice (Figure 1) when compared to sOva alone.
19 Though the antibody titers were still significant at 4 weeks p.i.
20 compared to sOva alone, we observed a slight decrease in titers
21 from 2 weeks to 4 weeks p.i. Our hypothesis is that the antigen-
22 containing micelles may facilitate crosslinking the B cell
23 receptor (BCR) and provide a rapid and low affinity antibody
24 response^{56,57}. This may be beneficial for presentation of the
25 antigen or a co-adjuvant to the receptors of immune cells in
26 orientations exposing certain conformational epitopes of the
27 antigen to crosslink multiple BCRs and provide an initial high
28
29
30
31
32
33
34
35
36
37
38
39
40
41
42
43
44
45
46
47
48
49
50
51
52
53
54
55

1
2
3 burst of antigen, resulting in rapid induction of antibody;
4
5 however, another adjuvant in combination with the micelles may be
6
7 required for induction of robust long-lasting immunity⁵⁸. We also
8
9 observed similar trends in enhancement of humoral immunity and
10
11 improved vaccine efficacy with influenza antigens 2 and 4 weeks
12
13 p.i. for PBC micelles alone and in combination with another vaccine
14
15 adjuvant, polyanhydride nanoparticles⁵⁴. We repeated the experiment
16
17 with Ova adjuvanted with micelles administered to BALB/c mice and
18
19 observed similar enhancement in antibody responses (data not
20
21 shown).
22
23
24

25
26 From previous studies, we had concluded that both the depot effect
27
28 formed by hydrogels and the outer cationic blocks of the polymer
29
30 contributed to enhanced antibody titers⁵⁵. Since the PBC micelle
31
32 concentration used in the present studies do not form a depot at
33
34 the injection site, unlike the hydrogels, we hypothesize that the
35
36 observed enhancement in humoral immunity may be attributed to the
37
38 association of the antigen and the PBC micelles. There is
39
40 significant interest in designing vaccine carriers to enhance
41
42 cytosolic uptake of antigens resulting in enhanced presentation
43
44 via the MHC I pathway and induction of CD8⁺ T cell responses^{53,59}.
45
46 In this context, pH-responsive polycationic gene delivery systems,
47
48 such as the PBC micelles, are known to translocate DNA from the
49
50 endosome to the cytosol by induction of the endosomal escape of
51
52
53
54
55
56
57
58
59
60

1
2
3 associated gene using a proton sponge effect^{15,60}. Hence, we studied
4
5 if these micelles associate with antigen in a similar manner and
6
7 deliver them to the cytosol.
8
9

10 We observed intracellular localization of the micelles and the
11 associated ovalbumin into the cytosol of both BMDCs and J774 cells
12 starting at an incubation period of 30 min and lasting until 12
13 hours (Figure 2, SI Figure 1 and 2). Ova is known to be
14
15 internalized after 15 min of incubation with APCs⁶¹. However, we
16
17 did not observe a significant amount of internalization by the
18
19 cells incubated with PBC micelles plus Ova in the first 15 min in
20
21 either BMDCs or J774 cells (SI Figure 2 and 3). Other studies have
22
23 shown that subsequently increasing amounts of Ova are detected
24
25 after 15 min in the cytosol due to endosomal escape caused by the
26
27 association with the carrier¹⁷. We showed association of Ova with
28
29 the PBC micelles by FRET, in which energy transfer between
30
31 fluorophores takes place in a non-radiative manner when they are
32
33 separated by a distance referred to as the Forster radius for the
34
35 two dyes (8.5 nm for our fluorophore system)⁶²⁻⁶⁴. We observed the
36
37 transfer of energy from donor to acceptor using the spectral
38
39 emission curve at specific concentrations of the antigen and the
40
41 micelles in solution (Figure 3). A similar technique was utilized
42
43 previously for studying complexation of DNA with the PBC
44
45 micelles^{37,65}. We utilized the same concentrations for studying FRET
46
47
48
49
50
51
52
53
54
55
56
57
58
59
60

1
2
3 *in vitro* with APCs using sensitized emission and a confocal
4 microscope. Even though we did not calculate the numerical value
5 of FRET efficiency, the FRET index image demonstrated the degree
6 of FRET occurring quantitatively. The areas of strong association
7 of the micelles with Ova as indicated by the FRET index image
8 (Figure 4) within the cytosol indicated that the micelles
9 transported the antigen to the cytosol. This hypothesis was
10 supported by the FACS analysis, which quantitatively demonstrated
11 enhanced uptake of Ova by BMDCs when associated with micelles
12 rather than when delivered alone. Starting at 60 min of incubation
13 with cells, the amount of Ova internalized steadily increased over
14 12 hours of incubation. (Figure 4C and SI Figure 3). It is also
15 worthwhile to note that we observed both stronger association of
16 micelles with Ova and enhanced uptake of Ova in BMDCs than in J774
17 cells. The micelles appeared to be localized more around the cell
18 membranes of the cells. Some studies have demonstrated that
19 amphiphilic molecules such as Pluronic can incorporate themselves
20 into the lipid bilayer of the membranes and facilitate protein
21 transport across it^{66,67}.

22
23 All these observations have particular relevance to the rational
24 design of vaccine formulations for older adults and
25 immunocompromised populations. The current strategy in commercial
26 vaccines for older adults (e.g., high dose Fluzone) is to deliver

1
2
3 four times the amount of vaccine dose as the normal dose. In this
4
5 context, the ability of the PBC micelles to increase the overall
6
7 antigen internalization can be beneficial for vaccine delivery in
8
9 older adults⁶⁸.

11 Many adjuvants or immune potentiators, including the licensed
12
13 adjuvant MPLA, act via the engagement of various receptors on
14
15 innate immune cells and their stimulation, which can be measured
16
17 by the upregulation of cell surface marker expression and cytokine
18
19 secretion⁶⁹. However, for PBC micelles, as demonstrated in Figure
20
21 5 and SI Figure 2, we did not observe any significant upregulation
22
23 of these markers. Therefore, it appears that these micelles do not
24
25 act as traditional immune stimulants or innate immune cell
26
27 activators, such as TLR ligands. Indeed, the activation of APCs
28
29 through TLRs may not always be desirable, especially when TLR
30
31 agonists induce excessive NO production, which can cause cellular
32
33 stress and contribute to acute inflammatory state of the immune
34
35 system^{49,70,71}. Higher amounts of NO production by inflammatory
36
37 immune cells has been linked to lower B cell activation, diminished
38
39 antibody responses, lower class-switching, and generation of more
40
41 short-lived plasma cells than long-lived plasma cells^{10,72}. In
42
43 contrast, administration of PBC micelles did not lead to the
44
45 production of NO or any cellular or mitochondrial ROS (Figure 7
46
47
48
49
50
51
52
53
54
55
56
57
58
59
60

1
2
3 and SI Figure 3) while still enhancing antibody production (Figure
4
5 1).

6
7 Finally, an analysis of the metabolic profile of APCs stimulated
8
9 with the PBC micelles demonstrated low mitochondrial stress when
10
11 compared to LPS (Figure 6). Rapid glycolytic activity as
12
13 demonstrated by the TLR agonists in extracellular flux analysis
14
15 has been reported to contribute to inflammation⁷³. In a separate
16
17 study using cathepsin activity, we have demonstrated that micelles
18
19 do not induce inflammation at the site of injection³¹. Combined
20
21 with the glycolytic activity of the micelles demonstrated in this
22
23 work (Figure 6), this suggests that a potential benefit of micelle
24
25 adjuvants would be to avoid adverse inflammatory reactions.
26
27
28
29

30 Overall, all these findings demonstrate that these PBC micelles,
31
32 while not activating APCs in a way that traditional TLR agonists
33
34 do, can still act as effective adjuvants for enhancing antibody
35
36 responses in the context of low inflammation and increasing antigen
37
38 trafficking into the cytosol of APCs. Given the enhanced
39
40 intracellular localization of antigen in the presence of the PBC
41
42 micelles, this observation is likely beneficial for designing an
43
44 effective vaccine regimen to enhance host immune responses that
45
46 have impaired APC functionality due to underlying inflammation and
47
48 potentially to induce cytotoxic T cell responses.
49
50
51
52
53
54
55
56
57
58
59
60

CONCLUSIONS

In this work, we demonstrated that a low concentration of an amphiphilic pentablock copolymer that undergoes pH sensitive micellization in aqueous solution can enhance adaptive immune responses in mice without forming a gel depot. We showed that the PBC micelles associate with antigens and deliver them to the cytosol of APCs. We also demonstrated that these PBC micelles are different from traditional TLR agonists in terms of their activation of APCs as evidenced by the lack of co-stimulatory molecule expression, cytokine secretion, induction of NO and ROS, and immunometabolic profiles. Therein, we found that PBC micelle-based nanoadjuvants do not generate mitochondrial stress and do not create a harmful inflammatory environment. These attributes make the PBC micelle adjuvants attractive candidates in the design of vaccines for older adults and immunocompromised patients.

Supporting Information Available

The following files are available free of charge:

Figure S1. Mean fluorescence intensity (MFI) of micelle-positive A) BMDCs and B) J774 cells. Cells were stimulated with 12.5 $\mu\text{g}/\text{mL}$ of PBC micelles labeled with AF647 for multiple time-points, washed and fixed in FACS buffer. Internalization was measured using flow

1
2
3 cytometry and the MFI was determined using FlowJo software. A
4 representative histogram demonstrating the shift in the cell
5 population treated with micelles (shown in gray, solid outline)
6 compared to control (shown in black, dotted outline) is shown for
7 C) BMDCs and D) J774 cells after 12-hour (720 min) incubation.
8 Data representative of three independent experiments and indicated
9 as mean with standard error of mean.
10
11
12
13
14
15
16
17
18
19

20 Figure S2. Trafficking of antigen into A) BMDCs and B) J774 cells
21 incubated for 15 min with pentablock copolymer (PBC) micelles (12.5
22 $\mu\text{g}/\text{mL}$) and antigen (20 $\mu\text{g}/\text{mL}$); C) BMDCs and D) J774 cells incubated
23 for 2 hours with PBC micelles and antigen. Cells seeded at a
24 concentration of 2.5×10^6 cells/mL on glass coverslips were
25 incubated with the micelles and ovalbumin for the required amount
26 of time. Scale bars indicate A) 50 μm and B), C) and D) 5 μm .
27 Nuclei were stained with Hoescht (blue). Ovalbumin antigen (AF594)
28 and PBC micelles (AF647) are denoted by red and cyan, respectively.
29 Data are representative of three independent experiments.
30
31
32
33
34
35
36
37
38
39
40
41
42

43 Figure S3. Time-course of the ovalbumin uptake when incubated with
44 pentablock copolymer (PBC) micelles for A) BMDCs and B) J774 cells.
45 The cells were incubated with the micelle-Ova complexes, micelle
46 formulation, Ova formulation and unstimulated control for the
47 indicated times and the protein mean fluorescence intensity (MFI)
48 was calculated using FlowJo software. Data represented as mean
49
50
51
52
53
54
55

1
2
3 with standard error of mean. **indicates statistical significance
4
5 determined using unpaired t-test with $p < 0.002$, $n = 3$
6
7

8 Figure S4. Pentablock copolymer (PBC) micelles did not show
9
10 significant upregulation of costimulatory molecules in bone marrow
11
12 macrophages and did not induce pro-inflammatory cytokine
13
14 secretion. BMMs at a concentration of 2.5×10^6 cells/mL were
15
16 stimulated for 48 hours with micelle or LPS (PBC micelles at the
17
18 concentration of $12.5 \mu\text{g/mL}$ and LPS at $1 \mu\text{g/mL}$). Cell surface
19
20 markers, MHCII, CD80 and CD40 upregulation were analyzed using
21
22 flow cytometry and cytokine secretion in supernatants were
23
24 analyzed using Multiplex bead assay. Data represented as mean with
25
26 standard error of mean. Statistical significance indicated by
27
28
29
30
31 ** $p < 0.005$ and *** $p < 0.0005$. $n = 3$.
32
33

34 Figure S5. PBC micelle adjuvants do not induce nitric oxide in
35
36 J774 cells and bone marrow macrophages. Cells were stimulated with
37
38 micelles and controls for 48 hours. Supernatants were collected to
39
40 analyze NO production using Griess assay. Data represented as mean
41
42 nitrite production with standard error of mean. **** indicates
43
44 statistical significance with $p < 0.0001$.
45
46
47
48
49

50
51 ACKNOWLEDGMENTS
52
53
54
55
56
57
58
59
60

1
2
3 The authors acknowledge funding from the National Institutes of Health (R01 AI127565-01 and
4 R01 AI141196-01) and the Iowa State University Nanovaccine Institute. Surya Mallapragada
5
6 and Balaji Narasimhan are grateful to the Carol Vohs Johnson Chair and the Vlasta Klima
7
8 Balloun Faculty Chair, respectively.
9
10
11
12
13
14
15
16
17
18
19
20
21
22
23
24
25
26
27
28
29
30
31
32
33
34
35
36
37
38
39
40
41
42
43
44
45
46
47
48
49
50
51
52
53
54
55
56
57
58
59
60

REFERENCES

1. Mallapragada SK, Narasimhan B. Immunomodulatory biomaterials. *Int J Pharm.* 2008;364(2):265-271.
doi:10.1016/j.ijpharm.2008.06.030.
2. Vartak A, Sucheck SJ. Recent Advances in Subunit Vaccine Carriers. Harper DM, Wall KA, eds. *Vaccines.* 2016;4(2):12.
doi:10.3390/vaccines4020012.
3. Kurella S, Manocha M, Sabhnani L, Thomas B, Rao DN. New age adjuvants and delivery systems for subunit vaccines. *Indian J Clin Biochem.* 2000;15(Suppl 1):83-100.
doi:10.1007/BF02867548.
4. Christensen D. Vaccine adjuvants: Why and how. *Hum Vaccin Immunother.* 2016;12(10):2709-2711.
doi:10.1080/21645515.2016.1219003.
5. Reed SG, Orr MT, Fox CB. Key roles of adjuvants in modern vaccines. *Nat Med.* 2013;19(12):1597-1608.
doi:10.1038/nm.3409.
6. Seder R, Reed SG, O'Hagan D, et al. Gaps in knowledge and prospects for research of adjuvanted vaccines. *Vaccine.* 2015. doi:10.1016/j.vaccine.2015.03.057.
7. Lee Y-TYY-J, Kim K-H, Ko E, et al. New vaccines against

- 1
2
3 influenza virus. *Clin Exp Vaccine Res.* 2014;3(1):12-28.
4
5 doi:10.7774/cevr.2014.3.1.12.
6
7
8
9 8. Haynes L, Swain SL. Commentary Why Aging T Cells Fail:
10 Implications for Vaccination. *Immunity.* 2006;24:663-666.
11
12 doi:10.1016/j.immuni.2006.06.003.
13
14
15
16 9. Fulop T, Larbi A, Dupuis G, et al. Immunosenescence and
17 Inflamm-Aging As Two Sides of the Same Coin: Friends or
18 Foes? *Front Immunol.* 2018;8:1960.
19
20
21
22 doi:10.3389/fimmu.2017.01960.
23
24
25
26 10. Giordano D, Draves KE, Li C, Hohl TM, Clark EA. Nitric Oxide
27 Regulates BAFF Expression and T Cell-Independent Antibody
28 Responses. *J Immunol.* 2014;193(3):1110-1120.
29
30
31
32 doi:10.4049/jimmunol.1303158.
33
34
35
36 11. Hubbell JA, Thomas SN, Swartz MA. Materials engineering for
37 immunomodulation. *Nature.* 2009;462:449.
38
39
40
41 <http://dx.doi.org/10.1038/nature08604>.
42
43
44 12. Yewdell JW. Designing CD8+ T Cell Vaccines: It's Not Rocket
45 Science (Yet). *Curr Opin Immunol.* 2010;22(3):402-410.
46
47
48
49 doi:10.1016/j.coi.2010.04.002.
50
51
52 13. Toit PB and VP and YEC and LC du. Stimuli-responsive
53 polymers and their applications in drug delivery. *Biomed*
54
55
56
57
58
59
60

- 1
2
3 *Mater.* 2009;4(2):22001. <http://stacks.iop.org/1748->
4
5 605X/4/i=2/a=022001.
6
7
- 8
9 14. Park TG, Jeong JH, Kim SW. Current status of polymeric gene
10 delivery systems. *Adv Drug Deliv Rev.* 2006;58(4):467-486.
11
12 doi:10.1016/J.ADDR.2006.03.007.
13
14
15
- 16 15. Foster S, Duvall CL, Crownover EF, Hoffman AS, Stayton PS.
17 Intracellular delivery of a protein antigen with an
18 endosomal-releasing polymer enhances CD8 T-cell production
19 and prophylactic vaccine efficacy. *Bioconjug Chem.*
20
21 2010;21:2205-2212. doi:10.1021/bc100204m.
22
23
24
25
26
27
- 28 16. Li Y-Y, Li L, Dong H-Q, Cai X-J, Ren T-B. Pluronic F127
29 nanomicelles engineered with nuclear localized functionality
30 for targeted drug delivery. 2013.
31
32 doi:10.1016/j.msec.2013.02.036.
33
34
35
36
37
- 38 17. Flanary S, Hoffman AS, Stayton PS. Antigen delivery with
39 poly (propylacrylic acid) conjugation enhances MHC-1
40 presentation and T-Cell activation. *Bioconjug Chem.*
41
42 2009;20(2):241-248. doi:10.1021/bc800317a.
43
44
45
46
47
- 48 18. Wilson JT, Keller S, Manganiello MJ, et al. PH-responsive
49 nanoparticle vaccines for dual-delivery of antigens and
50 immunostimulatory oligonucleotides. *ACS Nano.*
51
52 2013;7(5):3912-3925. doi:10.1021/nn305466z.
53
54
55
56
57
58
59
60

- 1
2
3 19. Agarwal A, Unfer R, Mallapragada SK. Novel cationic
4 pentablock copolymers as non-viral vectors for gene therapy.
5 *J Control Release*. 2005;103(1):245-258.
6
7 doi:10.1016/j.jconrel.2004.11.022.
8
9
10
11
12
13 20. Vogel BM, Mallapragada SK. Synthesis of novel biodegradable
14 polyanhydrides containing aromatic and glycol functionality
15 for tailoring of hydrophilicity in controlled drug delivery
16 devices. *Biomaterials*. 2005;26(7):721-728.
17
18 doi:10.1016/j.biomaterials.2004.03.024.
19
20
21
22
23
24
25 21. Adams JR, Mallapragada SK. Enhancing the immune response
26 through next generation polymeric vaccine adjuvants.
27 *Technology*. February 2014:1-12.
28
29 doi:10.1142/S2339547814300017.
30
31
32
33
34
35 22. Determan MD, Cox JP, Seifert S, Thiyagarajan P, Mallapragada
36 SK. Synthesis and characterization of temperature and pH-
37 responsive pentablock copolymers. *Polymer*. 2005;46:6933-
38 6946. doi:10.1016/j.polymer.2005.05.138.
39
40
41
42
43
44
45 23. Determan MD, Cox JP, Mallapragada SK. Drug release from pH-
46 responsive thermogelling pentablock copolymers. *J Biomed*
47 *Mater Res Part A*. 2007;81A(2):326-333.
48
49 doi:10.1002/jbm.a.30991.
50
51
52
53
54
55 24. Sahay G, Alakhova DY, Kabanov A V. Endocytosis of
56
57
58
59
60

- 1
2
3 nanomedicines. *J Control Release*. 2010;145(3):182-195.
4
5 doi:10.1016/J.JCONREL.2010.01.036.
6
7
- 8 25. Iversen T-G, Skotland T, Sandvig K. Endocytosis and
9
10 intracellular transport of nanoparticles: Present knowledge
11
12 and need for future studies. *Nano Today*. 2011;6(2):176-185.
13
14 doi:10.1016/J.NANTOD.2011.02.003.
15
16
- 17
18 26. Phanse Y, Lueth P, Ramer-Tait AE, et al. Cellular
19
20 internalization mechanisms of polyanhydride particles:
21
22 Implications for rational design of drug delivery vehicles.
23
24 *J Biomed Nanotechnol*. 2016;12(7):1544-1552.
25
26 doi:10.1166/jbn.2016.2259.
27
28
- 29
30 27. Hillaireau H, Couvreur P. Nanocarriers' entry into the cell:
31
32 relevance to drug delivery. *Cell Mol Life Sci*.
33
34 2009;66(17):2873-2896. doi:10.1007/s00018-009-0053-z.
35
36
37
- 38 28. Adams JR, Goswami M, Pohl NLB, Mallapragada SK. Synthesis
39
40 and functionalization of virus-mimicking cationic block
41
42 copolymers with pathogen-associated carbohydrates as
43
44 potential vaccine adjuvants. *RSC Adv*. 2014;4(30):15655.
45
46 doi:10.1039/c3ra47687a.
47
48
49
- 50 29. Adams JR, Haughney SL, Mallapragada SK. Acta Biomaterialia
51
52 Effective polymer adjuvants for sustained delivery of
53
54 protein subunit vaccines. *Acta Biomater*. 2015;14:104-114.
55
56

- 1
2
3 doi:10.1016/j.actbio.2014.11.050.
4
5
6 30. Ross K, Adams J, Loyd H, et al. Combination Nanovaccine
7
8 Demonstrates Synergistic Enhancement in Efficacy against
9
10 Influenza. *ACS Biomater Sci Eng*. 2016; 2(3): 368-374.
11
12 doi:10.1021/acsbiomaterials.5b00477.
13
14
15
16 31. Adams, Justin R., Sujata Senapati, Shannon L. Haughney,
17
18 Michael J. Wannemuehler, Balaji Narasimhan SM. Safety and
19
20 biocompatibility of injectible vaccine adjuvants composed of
21
22 thermogelling block copolymer gels. *Submitt to J Biomed*
23
24 *Mater Res*. 2018.
25
26
27
28 32. Adams JR, Mallapragada SK. Novel Atom Transfer Radical
29
30 Polymerization Method to Yield Copper-Free Block Copolymeric
31
32 Biomaterials. *Macromol Chem Phys*. 2013;214(12):1321-1325.
33
34 doi:10.1002/macp.201300034.
35
36
37
38 33. Petersen LK, Xue L, Wannemuehler MJ, Rajan K, Narasimhan B.
39
40 The simultaneous effect of polymer chemistry and device
41
42 geometry on the in vitro activation of murine dendritic
43
44 cells. *Biomaterials*. 2009;30(28):5131-5142.
45
46 doi:http://dx.doi.org/10.1016/j.biomaterials.2009.05.069.
47
48
49
50 34. Hass M H, Noel C, Marchal O, Matthes H, Gloria S, Galzi JL.
51
52 FRET and Colocalization Analyzer—A Method to
53
54 ValidateMeasurements of Sensitized Emission FRET Acquired

- 1
2
3 byConfocal Microscopy and Available as an ImageJ Plug-in.
4
5 *Microsc Res Tech.* 2006;69:941-956.
6
7 doi:http://onlinelibrary.wiley.com/doi/10.1002/jemt.20376/ep
8
9 df.
10
11
12
- 13 35. Arsov Z, Švajger U, Mravljak J, et al. Internalization and
14
15 Accumulation in Dendritic Cells of a Small pH-Activatable
16
17 Glycomimetic Fluorescent Probe as Revealed by Spectral
18
19 Detection. *ChemBioChem.* 2015;16(18):2660-2667.
20
21 doi:10.1002/cbic.201500376.
22
23
- 24
25 36. Tomić S, Đokić J, Vasilijić S, et al. Size-Dependent Effects
26
27 of Gold Nanoparticles Uptake on Maturation and Antitumor
28
29 Functions of Human Dendritic Cells In Vitro. Hussain S, ed.
30
31 *PLoS One.* 2014;9(5):e96584.
32
33 doi:10.1371/journal.pone.0096584.
34
35
- 36
37 37. Jia F, Zhang Y, Narasimhan B, Mallapragada SK. Block
38
39 copolymer-quantum dot micelles for multienzyme
40
41 colocalization. *Langmuir.* 2012;28(50):17389-17395.
42
43 doi:10.1021/la303115t.
44
45
- 46
47 38. Bobryshev Y V., Karagodin VP, Orekhov AN. Dendritic cells
48
49 and their role in immune reactions of atherosclerosis. *Cell*
50
51 *tissue biol.* 2013;7(2):113-125.
52
53 doi:10.1134/S1990519X1302003X.
54
55

60

- 1
2
3 39. van Vliet SJ, García-Vallejo JJ, van Kooyk Y. Dendritic
4 cells and C-type lectin receptors: coupling innate to
5
6 adaptive immune responses. *Immunol Cell Biol.*
7
8 2008;86(7):580-587. doi:10.1038/icb.2008.55.
9
10
11
12
13 40. Petersen LK, Ramer-Tait AE, Broderick SR, et al. Activation
14 of innate immune responses in a pathogen-mimicking manner by
15
16 amphiphilic polyanhydride nanoparticle adjuvants.
17
18 *Biomaterials.* 2011;32(28):6815-6822.
19
20 doi:10.1016/j.biomaterials.2011.05.063.
21
22
23
24
25 41. Thwe PM, Amiel E. The role of nitric oxide in metabolic
26
27 regulation of Dendritic cell immune function. *Cancer Lett.*
28
29 2018;412:236-242. doi:10.1016/j.canlet.2017.10.032.
30
31
32
33 42. Everts B, Pearce EJ. Metabolic control of dendritic cell
34
35 activation and function: Recent advances and clinical
36
37 implications. *Front Immunol.* 2014;5(MAY):203.
38
39 doi:10.3389/fimmu.2014.00203.
40
41
42
43 43. O'Neill LAJ, Pearce EJ. Immunometabolism governs dendritic
44
45 cell and macrophage function. *J Exp Med.* 2016;213(1):15-23.
46
47 doi:10.1084/jem.20151570.
48
49
50
51 44. Krawczyk CM, Holowka T, Sun J, et al. Toll-like receptor-
52
53 induced changes in glycolytic metabolism regulate dendritic
54
55 cell activation. *Blood.* 2010;115(23):4742-4749.
56
57
58
59
60

- 1
2
3 doi:10.1182/blood-2009-10-249540.
4
5
6
7 45. Everts B, Amiel E, Van Der Windt GJW, et al. Commitment to
8 glycolysis sustains survival of NO-producing inflammatory
9 dendritic cells. *Blood*. 2012;120(7):1422-1431.
10
11 doi:10.1182/blood-2012-03-419747.
12
13
14
15
16 46. Everts B, Amiel E, Huang SCC, et al. TLR-driven early
17 glycolytic reprogramming via the kinases TBK1-IKK ϵ supports
18 the anabolic demands of dendritic cell activation. *Nat*
19
20
21
22
23
24
25
26 47. Kanof ME. Isolation of T Cells Using Rosetting Procedures.
27
28 2016:1-5. doi:10.1002/0471142735.im0702s112.
29
30
31 48. Serbina N V., Salazar-Mather TP, Biron CA, Kuziel WA, Pamer
32 EG. TNF/iNOS-producing dendritic cells mediate innate immune
33
34
35
36
37
38
39
40
41
42
43
44
45
46
47
48
49 49. Bogdan C. Nitric oxide synthase in innate and adaptive
50
51
52
53
54
55
56
57
58
59
60
- immunity: An update. *Trends Immunol*. 2015;36(3):161-178.
doi:10.1016/j.it.2015.01.003.
50. Wilson-Welder JH, Torres MP, Kipper MJ, Mallapragada SK,
Wannemuehler MJ, Narasimhan B. Vaccine adjuvants: Current
challenges and future approaches. *J Pharm Sci*.

- 1
2
3 2009;98(4):1278-1316.
4
5 doi:http://dx.doi.org/10.1002/jps.21523.
6
7
8
9 51. Brito LA, O'Hagan DT. Designing and building the next
10 generation of improved vaccine adjuvants. *J Control Release*.
11 2014;190:563-579. doi:10.1016/j.jconrel.2014.06.027.
12
13
14
15
16 52. Narasimhan B, Goodman JT, Vela Ramirez JE. Rational Design
17 of Targeted Next-Generation Carriers for Drug and Vaccine
18 Delivery. *Annu Rev Biomed Eng*. January 2016.
19
20
21
22 doi:10.1146/annurev-bioeng-082615-030519.
23
24
25
26 53. O'Hagan DT, Fox CB. New generation adjuvants - From
27 empiricism to rational design. *Vaccine*. 2015;33(S2):B14-B20.
28
29
30
31 doi:10.1016/j.vaccine.2015.01.088.
32
33
34 54. Ross K, Adams J, Loyd H, et al. Combination Nanovaccine
35 Demonstrates Synergistic Enhancement in Efficacy against
36 Influenza. *ACS Biomater Sci Eng*. 2016;2(3):368-374.
37
38
39
40
41 doi:10.1021/acsbiomaterials.5b00477.
42
43
44 55. Adams JR, Haughney SL, Mallapragada SK. Effective polymer
45 adjuvants for sustained delivery of protein subunit
46 vaccines. *Acta Biomater*. 2015;14:104-114.
47
48
49
50
51 doi:http://dx.doi.org/10.1016/j.actbio.2014.11.050.
52
53
54 56. Hitomi T, Yanagi S, Inatome R, Yamamura H. Cross-linking of
55
56
57
58
59
60

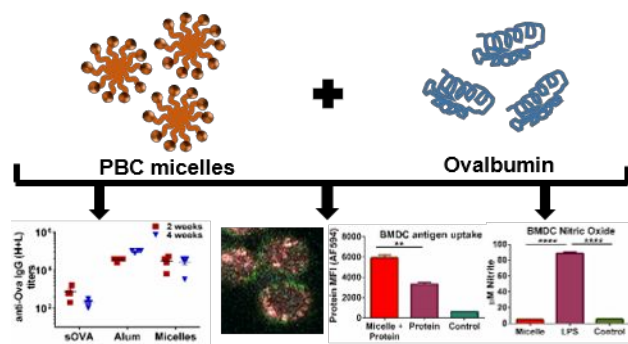
- 1
2
3 the B cell receptor induces activation of phospholipase D
4 through Syk, Btk and phospholipase C- γ 2. *FEBS Lett.*
5
6 1999;445(2-3):371-374. doi:10.1016/S0014-5793(99)00153-2.
7
8
9
10
11 57. Liu W, Sohn HW, Tolar P, Pierce SK. It's all about change:
12 the antigen-driven initiation of B-cell receptor signaling.
13 *Cold Spring Harb Perspect Biol.* 2010;2(7):a002295.
14
15 doi:10.1101/cshperspect.a002295.
16
17
18
19
20
21 58. Ross K, Senapati S, Alley J, et al. Single dose combination
22 nanovaccine provides protection against influenza A virus in
23 young and aged mice. *Biomater Sci.* 2019.
24
25 doi:10.1039/C8BM01443D.
26
27
28
29
30
31 59. Zacharias ZR, Ross KA, Hornick EE, et al. Polyamide
32 Nanovaccine Induces Robust Pulmonary B and T Cell Immunity
33 and Confers Protection Against Homologous and Heterologous
34 Influenza A Virus Infections. *Front Immunol.* 2018;9:1953.
35
36 doi:10.3389/fimmu.2018.01953.
37
38
39
40
41
42
43 60. Yong Woo Cho J-DK and KP. Polycation gene delivery systems:
44 escapes from endosome to cytosol. *J Pharm Pharmacol.*
45
46 2003;55:721-734. doi:10.1211/0022357021206.
47
48
49
50
51 61. Platt CD, Ma JK, Chalouni C, et al. Mature dendritic cells
52 use endocytic receptors to capture and present antigens.
53
54 *Proc Natl Acad Sci U S A.* 2010;107(9):4287-4292.
55
56

- 1
2
3 doi:10.1073/pnas.0910609107.
4
5
6 62. Gravier J, Sancey L, Hirsjärvi S, et al. FRET imaging
7
8 approaches for in vitro and in vivo characterization of
9
10 synthetic lipid nanoparticles. *Mol Pharm*. 2014;11(9):3133-
11
12 3144. doi:10.1021/mp500329z.
13
14
15
16 63. Sekar RB, Periasamy A. Fluorescence resonance energy
17
18 transfer (FRET) microscopy imaging of live cell protein
19
20 localizations. *J Cell Biol*. 2003;160(5):629-633.
21
22 doi:10.1083/jcb.200210140.
23
24
25
26 64. Morton SW, Zhao X, Quadir MA, Hammond PT. Biomaterials FRET-
27
28 enabled biological characterization of polymeric micelles.
29
30 *Biomaterials*. 2014;35(11):3489-3496.
31
32 doi:10.1016/j.biomaterials.2014.01.027.
33
34
35
36 65. Zhang B, Zhang Y, Mallapragada SK, Clapp AR. Sensing Polymer
37
38 / DNA Polyplex Fluorophores. 2011;5(1):129-138.
39
40
41
42 66. Gaurav S, Elena VB, Alexander VK. Different internalization
43
44 pathways of polymeric micelles and unimers and their effects
45
46 on vesicular transport. *Bioconjug Chem*. 2013;19(1):51-57.
47
48 doi:10.1016/j.jconrel.2012.01.032.Sustained.
49
50
51 67. Kabanov A V., Levashov A V., Alakhov VY. Lipid modification
52
53 of proteins and their membrane transport. *Protein Eng Des*
54
55

- 1
2
3 *Se1*. 1989;3(1):39-42. doi:10.1093/protein/3.1.39.
4
5
6
7 68. Centers for Disease Control and Prevention. Fluzone High-
8 Dose Seasonal Influenza Vaccine.
9
10 https://www.cdc.gov/flu/protect/vaccine/qa_fluzone.htm.
11
12
13
14 69. Flower DR. Systematic identification of small molecule
15 adjuvants. *Expert Opin Drug Discov*. 2012;7(9):807-817.
16 doi:10.1517/17460441.2012.699958.
17
18
19
20
21 70. Sun J, Zhang X, Broderick M, et al. Measurement of Nitric
22 Oxide Production in Biological Systems by Using Griess
23 Reaction Assay. *Sensors*. 2003;3(8):276-284.
24 doi:10.3390/s30800276.
25
26
27
28
29
30
31 71. Stuehr DJ, Marletta MA. Mammalian nitrate biosynthesis:
32 mouse macrophages produce nitrite and nitrate in response to
33 *Escherichia coli* lipopolysaccharide. *Proc Natl Acad Sci*.
34 1985;82(22):7738 LP-7742.
35 <http://www.pnas.org/content/82/22/7738.abstract>.
36
37
38
39
40
41
42
43 72. Sammiceli S, Kuka M, Di Lucia P, et al. Inflammatory
44 monocytes hinder antiviral B cell responses. *Sci Immunol*.
45 2016;1(4):1-11. doi:10.1126/sciimmunol.aah6789.
46
47
48
49
50
51 73. Pence BD, Yarbrow JR. Aging impairs mitochondrial respiratory
52 capacity in classical monocytes. *Exp Gerontol*. 2018;108:112-
53
54
55

117. doi:10.1016/J.EXGER.2018.04.008.

For Table of Contents Use Only



Pentablock copolymer micelle nanoadjuvants enhance cytosolic delivery of antigen and improve vaccine efficacy while inducing low inflammation

Sujata Senapati^{1,4}, Ross J. Darling^{2,4}, Darren Loh³, Ian C. Schneider^{1,4}, Michael J. Wannemuehler^{2,4}, Balaji Narasimhan^{1,4*}, and Surya K. Mallapragada^{1,4,*}

¹Department of Chemical and Biological Engineering, Iowa State University, Ames, IA, 50011, USA

²Department of Veterinary Microbiology and Preventive Medicine, Iowa State University, Ames, IA, 50011, USA

³Department of Chemical and Biological Engineering, Johns Hopkins University, Baltimore, MD, 21218, USA

1
2
3 ⁴Nanovaccine Institute, Iowa State University, Ames, IA, 50011,
4
5 USA

6
7
8 *Correspondence:

9
10
11 Surya Mallapragada (suryakm@iastate.edu) and Balaji Narasimhan (nbalaji@iastate.edu)
12
13
14
15
16
17
18
19
20
21
22
23
24
25
26
27
28
29
30
31
32
33
34
35
36
37
38
39
40
41
42
43
44
45
46
47
48
49
50
51
52
53
54
55
56
57
58
59
60